Precise Segmentation Rendering for Medical Images Based on Maximum Entropy Processing

Tsair-Fwu Lee[1,2], Ming-Yuan Cho[1], Chin-Shiuh Shieh[4], Pei-Ju Chao[3], and Huai-Yang Chang[2]

[1] Department of Electrical Engineering, National Kaohsiung University of Applied Science, Kaohsiung, Taiwan 807, ROC
[2] Department of Radiation Oncology, Chang Gung Memorial Hospital-Kaohsiung, 83305, Taiwan, ROC
[3] Department of Radiation Oncology, Kaohsiung Yuan's General Hospital, Kaohsiung, 800, Taiwan, ROC
[4] Department of Electronic Engineering, National Kaohsiung University of Applied Science, Kaohsiung, Taiwan 807, ROC

Abstract. Precision is definitely required in medical treatments, however, most three-dimensional (3-D) renderings of medical images lack for required precision. This study aimed at the development of a precise 3-D image processing method to discriminate clearly the edges. Since conventional Computed Tomography (CT), Positron Emission Tomography (PET), or Magnetic Resonance Imaging (MRI) medical images are all slice-based stacked 3-D images, one effective way to obtain precision 3-D rendering is to process the sliced data with high precision first then to stack them together carefully to reconstruct a desired 3-D image. A recent two-dimensional (2-D) image processing method known as the entropy maximization procedure proposed to combine both the gradient and the region segmentation approaches to achieve a much better result than either alone seemed to be our best choice to extend it into 3-D processing. Three examples of CT scan data of medical images were used to test the validity of our method. We found our 3-D renderings not only achieved the precision we sought but also has many interesting characteristics that shall be of significant influence to the medical practice.

Keywords: segmentation, wavelet, edge detection, entropy maximization.

1 Introduction

Physicians need 3-D renderings to help them to make diagnosis, conduct surgery, and provide other treatments that 2-D images and other conventional test methods cannot offer. Without precise segmentation, renderings could lead to misleading results. The aim of this study is to provide a precise 3-D rendering method to achieve what physicians demand. Two basic approaches in existing works on image segmentation are: the gradient-based approach and the region-based approach. Gradient-based edge detection methods [1,2] rely on the local

R. Khosla et al. (Eds.): KES 2005, LNAI 3683, pp. 366–373, 2005.

differences in the gray scale values of an image. They focus on the differences and transitions of the intensity of an image. The disadvantage in these methods is that they almost always result in broken and false edges. Region-based segmentation techniques include region-growing, region-splitting, and region-merging algorithms, *etc.* focused on the homogeneity of spatially dense localized features and other pixel statistics. They have a common problem of over-segmented, and hence produces poorly localized region boundaries. To resolve their weaknesses and to combine their strengths of the gradient-based approach and the region-based approach, Staib and Duncan proposed an idea to combine both of them in the maximum entropy manner to achieve a better result [3,4]. And recently Duncan *et al.* [5] have some successful applications in its extented works. Moreover, some authors paid more attention in this field with different methods in progress [6].

In this study, our objective is to apply the Staib and Duncan method [3,4] to combine various segmentation approaches with an entropy maximization procedure and extended the idea into 3-D area. This allows us to utilize all available information to achieve the most robust segmentation results for 3-D image processing. We then apply our combined segmentation method to medical images to test the validity of our method. We aim to show our combined 3-D segmentation method is indeed superior in terms of required precision, also the sliced-base approach we proposed is quite efficient, and many features generated by our 3-D segmentation method shall be of referential values to the physicians.

2 Wavelet Edge Detector

No doubt the Wavelet method is known to be one of the best gradient segmentation methods due to its multi-scale and multi-resolution capabilities. We briefly discuss some of its property in this section. We shall name $S_{2^j}[.]$ and $D_{2^j}[.]$ as the low pass signal (or the approximated signal) and the high pass signal (or the detailed signal) of $f(x)$ at resolution 2^j**,** respectively. And $S_{2^j}[n]$ is the projection coefficient of $f(x)$ on subspace V_j, $D_{2^j}[n]$ is the projection coefficient of $f(x)$ on subspace O_j.We can define an orthogonal complement subspace of V_j as O_j, in space V_{j+1}. The scaling function $\phi(x)$ and wavelet function $\varphi(x)$ have the orthogonal properties. From the properties of multiresolution analysis, we can easily see that signals can always be decomposed into higher resolutions until the desired result is obtained. A 2-D filter for edge detection is generated by a 2-D discrete periodic wavelet transform (2-D DPWT) [4], applying separable algorithms, the 2-D DPWT can be written in a matrix form. And we now extend the wavelet transform into two dimensional manners. So we can define the four operators [4,7] of 2-D DPWT as follows: (Reader can refer to the detail description in the reference [8] which proposed by Mallat in 1989.)

$$W_{LL} = [h(i) \cdot h(j)]_{i,j \in Z} \tag{1}$$

$$W_{LH} = [(-1)^{3-j} h(i) \cdot h(3-j)]_{i,j \in Z} \tag{2}$$

$$W_{HL} = [(-1)^{3-j} h(3-i) \cdot h(j)]_{i,j \in Z} \tag{3}$$

$$W_{HH} = [(-1)^{i+j} h(3-i) \cdot h(3-j)]_{i,j \in Z} \tag{4}$$

where, W_{LL}, W_{LH}, W_{HL} and W_{HH} are the four subband filters; and the $\otimes$ denoted a convolution operation; and $h(i) =< \phi_{2^{-1}}(u) \cdot \phi(u-i) >$. Clearly, as the length of the coefficients of the filter is d, the operator of 2-D DPWT formed a $d \times d$ matrix. We now use the coefficients of the four filters given by Eq. 1 to Eq. 4 to generate a wavelet edge detector. Let $f_h(i,j)$ be the horizontal high-pass filter function and $f_v(i,j)$ be the vertical high-pass filter function. These two high-pass filters are obtained from the four operators of 2-D DPWT

$$f_h(i,j) = W_{LL}(i,j) \otimes W_{LH}(i,j) \tag{5}$$

$$f_v(i,j) = W_{LL}(i,j) \otimes W_{HL}(i,j). \tag{6}$$

We then apply the different length coefficients of Daubechies wavelet transform to generate the multi-scale masks (filters)[4,7,8].

Therefore, let the original image pass through these masks to produce a series of multi-scale images with different gradient strength scales. In order to avoid distortions caused by noise and to define exact edge points, an edge thinning technique is then used to make effective combinations of the images [9].

3 Concepts of Maximum Entropy Processing

By boundary estimation we meant to find optimum values of the boundary parameters as the information of image data were given. Let us define the optimization of the entropy function by maximizing its *a posteriori* probability (MAP) [3,10]. Assuming that $I_b(x,y)$ is the image that depicts some object and $t_{\hat{p}}(x,y)$ is the image template corresponding to the parameter vector $\hat{p}$. We maximize $P(t_{\hat{p}}|I_b)$, the conditional probability of the template given the image, to obtain the best estimate of $\hat{p}$. By Baye's rule, the function $P(t_{\hat{p}}|I_b)$ can be written as follows:

$$\arg\max_{\hat{p}} P(t_{\hat{p}}|I_b) = \arg\max_{\hat{p}} \frac{P(I_b|t_{\hat{p}})P(t_{\hat{p}})}{P(I_b)} \tag{7}$$

where $P(t_{\hat{p}})$ is the *a priori* probability of the template and $P(I_b|t_{\hat{p}})$ is the conditional probability of image I_b, which depicts some object with template $\hat{p}$. The denominator of Eq. 7 is not a function of $\hat{p}$ and hence can be ignored. Taking logarithm of Eq. 7 we have:

$$\arg\max_{\hat{p}} M(I_b, t_{\hat{p}}) = \arg\max_{\hat{p}} [lnP(t_{\hat{p}}) + lnP(I_b|t_{\hat{p}})] \tag{8}$$

To estimate the parameter vector $\hat{p}$ we maximize the entropy function $M(I_b, t_{\hat{p}})$. Clearly, the first term of Eq. 8 represents the *a priori* information and the second term represents the data-driven likelihood term. After rearranged the equation by Baye's rule, we find the boundary estimation problem becomes

$$\arg\max_{\hat{p}} ln[P(\hat{p}|I_g, I_r)] \equiv \arg\max_{\hat{p}} [lnP(\hat{p}) + lnP(I_g|\hat{p}) + lnP(I_r|(I_g, \hat{p})] \tag{9}$$

Clearly, the first term is the *a priori* information, the second term contains the gradient-based information I_g, and the last term is the region-based informationI_r

conditioned on parameter vector $\hat{p}$ and the gradient-based information I_g. We argue that we shall ignore the dependence on I_g since the information of gradient-based information is already obtained by the second term. Then Eq. 9 becomes

$$\arg\max_{\hat{p}} M(\hat{p}, I_g, I_r) \equiv \arg\max_{\hat{p}}[M_{prior}(\hat{p}) + M_{gradient}(I_g, \hat{p}) + M_{region}(I_r, \hat{p})] \tag{10}$$

For each slice, the input consists of the original image I and the region-classified image I_r which is the result of region-based segmentation as discussed above. Next a gradient-based approach is added and it uses the gradient image I_g. As described by Staib and Duncan [3,10], we shall use the magnitude of the gradient vector at each voxel location. I_g can be obtained from I either by convolving the input image I with the multiple wavelet edge detection operators and then computing I_g to be the magnitude of the above resulting vector image. Hence the input to the system is the gradient image I_g and the region-classified image I_r. Only when slice processing is completed, we use linear interpolation algorithm along the slices direction to form 3-D surfaces. We argue that, our surface estimation method using both gradient and region homogeneity information is still in the maximum *a posteriori* framework. We have suitably incorporated *a priori* shape information when region-of-interest (ROI) is available.

4 Medical Images Applications and Results

The goal of our precise image segmentation is to partition an image into disjoint regions of desired objects as accurate as possible. Among the proposed segmentation methods, region-growing has been the most popular one due to its speed and great flexibility. We use symmetric seeds [11] to initiate the segmentation to avoid a single seed may fall into a noise region too easily. Then we combine the region-growing segmentation with the gradient-based segmentations, namely the wavelet edge detector. The following are precision 3-D renderings generated by our combine-information segmentation applies to medical images of distinct characteristics and medical importance.

4.1 Medical Image Experiment 1

A set of CT scan, slices of a human chest which we want to process only a particular region of medical interests. This also demonstrated the great capability and flexibility of our combine-information segmentation method.

We find the edges by following the boundary-finding procedure. The gradient-based information is obtained first by using the wavelet edge detection method, and the region-based information is obtained from the region-growing method initialized with symmetric seeds. The entropy function Eq. 10 completes the combination in maximum sense. As we have discussed earlier, when we process the gradient-based information only, the first two terms are used as entropy functions. As we process the image with the region-based information only, we used the first and the third terms as entropy functions. Finally, all three terms are used as entropy functions to complete the combination. We shall perform the segmentation first slice by slice. Since we aim to extract the right lung for feature

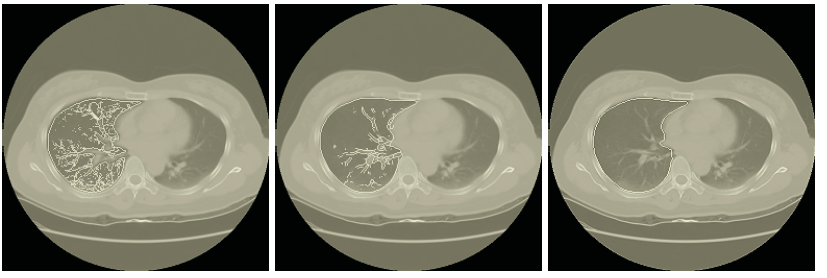

(a) (b) (c)

Fig. 1. (a) Segmented contour by the region-growing method. (b) Segmented contour by the wavelet method. (c) Segmented contour by the combination method

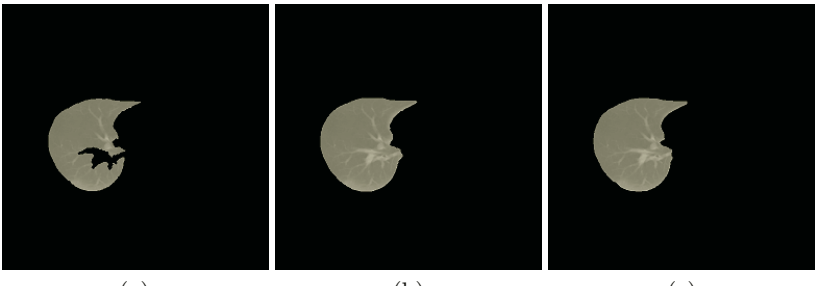

(a) (b) (c)

Fig. 2. (a) Segmented result of the region-growing method.(b) Segmented result of the wavelet method. (c) Segmented result of the combination method

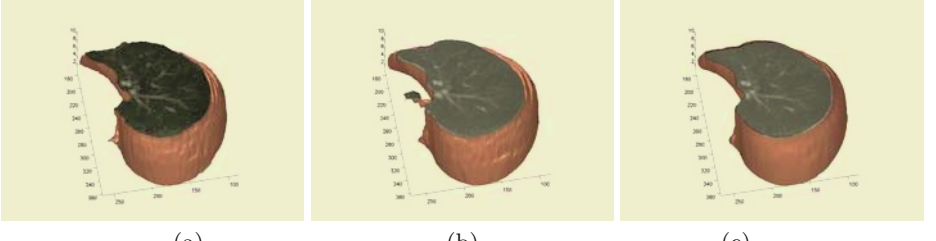

(a) (b) (c)

Fig. 3. (a) 3-D rendering by the region-growing method. (b) 3-D rendering by wavelet method. (c) 3-D rendering by the combination method

extraction in this case hence it becomes our natural ROI. Fig. 1 (a) shown the region-growing contour, Fig. 1 (b) is the wavelet contour, and Fig. 1 (c) is the combined contour. Figs. 2 (a) (b) and (c) present the segmentation results of Figs. 1 (a) (b) and (c) respectively. On close inspection of these figures, shortcomings from either segmentation although were obvious but seemed harmless. However, as 3-D renderings were form, they become serious errors, and shall not be tolerated if precision renderings were sought.

Fig. 3 (a) shows the 3-D rendering from the region-growing segmentation. Fig. 3 (b) shows the 3-D rendering from the wavelet segmentation. Fig. 3 (c) shows

the 3-D rendering from the combined segmentation. If we look at them closely, we found that the 3-D renderings either by the region-growing segmentation, or by the wavelet segmentations, although seemed both acceptable, but they both have problems that at times a single slice will be very different from the others at some particular point, perhaps due to noise and/or other disturbances, which makes the corresponding 3-D renderings appeared with wrinkles. Clearly human lungs should be continuous and smooth in all directions always, hence we may conclude that both the region-growing method and the wavelet method fail to reconstruct the object precisely.

As expected, the maximum entropy combination results in a 3-D rendering with much better quality. Hence we can conclude that the combined method is indeed superior to each individual processing alone, and our purpose of seeking precision has been achieved.

4.2 Medical Image Experiment 2

Next we shall test the accuracy of localization of our method. By the use of coloring and a so-called transparency technique, not only we can identify the problem area precisely, but also its relative position to other critical organs. The test data were the CT scan of a female patient with a pituitary tumor in her brain. The pituitary gland is about the size of a pea in the center of our brain just at the back of our nose. The choice of treatment uniquely depends on the position of the tumor.

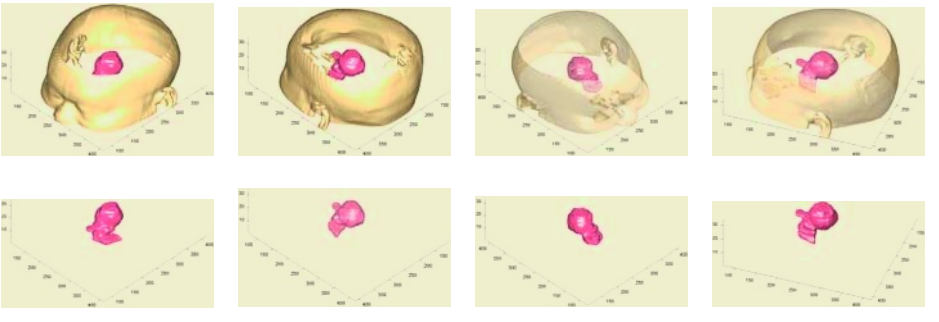

Fig. 4. 3-D renderings of the tumor and the head in two colors, four angles, and transparent effect

Here we emphasize the importance of precision. With a target so small and so vital, only position of the tumors can be pin down with the highest precision, treatments can then be effective, and ordinary brain cells shall not be damage.

In order to identify the tumor clearly, we first segmented it out with great precision and then 3-D renderings of the pituitary tumor are then constructed. The tumor can now be clearly inspected by checking the Fig.4. The figures clearly demonstrated the power of our segmentation, capable of providing an outstanding positioning of the tumor, which has not been achieved by other 3-D

renderings previously. The size and shape of the tumor, its orientation with the brain, and the position relative to the head are all now clearly seen.Its various angles are shown in the Figs. These 3-D renderings can be rotated to any angle and with different colors for physicians to inspect closely. Transparency effect is now introduced which shall be most useful for radiation therapies.

4.3 Medical Image Experiment 3

Finally we shall present the 3-D renderings for a common orthopedic decease happens to both genders for senior citizens. Human stands on two feet and the joint between our legs and our pelvis solely supports our weight. In medical terms, it is the femur connecting to the acetabulum supporting our weight. Over years of overly use, the joint becomes rough and causes pain. If it is not taken care of properly, fragment shall occur. How were the joint over used, what are the damages, in present days orthopedic surgeon either depends on CT scan or inspect by endoscopes. However, endoscopes inspection is time consuming; CT slices although were the best X-ray scan able to provide, really did not fully expose the problem.

(a) (b) (c) (d)

Fig. 5. (a) 3-D rendering of the pelvis. (b) (c) 3-D renderings of the right joint in different angle. (d) The pelvis with transparent effect in different angle

(a) (b) (c) (d)

Fig. 6. (a) 3-D rendering of the acetabulum in pelvis. (b) The acetabulum in pelvis in a different angle. (c) (d) 3-D renderings of the femur in different angles

With the reconstruction techniques we have developed, precision 3-D renderings of all angles, enlargements, distinct part of the joint, can all be visualize much clearly allowing physicians to make correct decisions. Fig. 5 (a) shows the pelvis only for physicians to inspect in detail. Fig. 5 (b) (c) shows the complete right joint of the pelvis in different angles. Figs. 5 (d) showed its different angle with transparent effect to simulate various movements of the joint. Figs. 6 (a)

and (b) are the close look of the acetabulum. Fig. 6 (c) (d) shows the different angle of the femur. With the help of these 3-D renderings, physicians shall be able to make diagnosis more efficiently and effectively.

5 Conclusion

On all examples of medical images we processed, not only desired precision had been achieved, we are also able to create rotation of the objects to obtain its 3-D images of different angles. The 3-D renderings we created will allow physicians to conduct surgery or treatment much more accurately and effectively. Many images of interest that physicians unable to visualize, but have to compose a 3-D image by their imaginations, all become possible after our 3-D processing. Features are now clearly identified, locations pinned down exactly, and relative orientations are now well understood. These are all vital for medical treatments.

Therefore we may conclude that our 3-D rendering method that combines the gradient-based and the region-based information in the maximum entropy sense, not only proved to be a superb image processing techniques but also very useful in practice for medical images. We believe that our precision 3-D renderings shall play its role in future medical applications.

References

1. John C. Russ. The Image Processing Handbook, Third ed. CRC Press & IEEE Press, 1999.
2. Rafael C. Gonzalez, Richard E. Woods. Digital Image Processing. Prentice Hall, 2^{nd} ed. Edition, 2002.
3. L.H. Staib. "Boundary finding with parametrically deformable models." *IEEE Transactions on Pattern Analysis and Machine Intelligence*, vol.14, no.11, pp.1061-1075, 1992.
4. Cheng-Tung Ku, King-Chu Hung and Mig-Cheg Liag. "Wavelet Operators for Multi-scale Edge and Corner Detection." Department of Electrical Engineering, I-Shou University, Taiwan, 1998.
5. Jing Yang, James S. Duncan. "Joint Prior Models of Neighboring Objects for 3D Image Segmentation", Proceedings of the 2004 IEEE Computer Society Conference on Computer Vision and Pattern Recognition (CVPR'04), 1063-6919/04,2004.
6. Hua Li, Abderr Elmoataz, Jalal Fadili, Su Ruan, Barbara Romaniuk. "3D Medical Image Segmentation Approach Based on Multi-Label Front Propagation ", IEEE 2004 International Conference on Image Processing (ICIP), pp. 2925-2928, 2004.
7. Yih-Sheng Leu, Chao-Ji Chou. "Wavelet Edge Detection on Region-based Image Segmentation" Department of Computer & Communication Engineering, National Kaohsiung First University of Science and Technology, Taiwan, 2000.
8. S.G. Mallat, "A Theory for Multiresolution Signal Decomposition: The Wavelet Representation." *IEEE Transactions on Analysis and Machine Intelligence*, vol. 11. no. 7, 1989.
9. Gabriele Lohmann. Volumetric Image Analysis. Wiley & Teubner, 1998.
10. A. Chakraborty, "Feature and Module Integration for Image Segmentation." Ph.D thesis, Yale University, 1996.
11. Shu-Yen Wan, William E. Higgins. "Symmetric Region Growing." *IEEE Transactions on image processing*, vol. 12, no.9, pp 1007-1015, September 2003.